WHAT DO BINARIES TEACH US ABOUT MASS-LOSS FROM LATE-TYPE STARS ?

Dieter Reimers
Hamburger Sternwarte, Universität Hamburg
Gojenbergsweg 112, 2o5o Hamburg 8o
Federal Republic of Germany

ABSTRACT. It is shown that the binary technique - a B star companion is used as a light source which probes the wind of the red giant primary - has yielded accurate mass-loss rates and wind velocities for 8 G to M (super)giants and (in some cases) estimates of wind temperature.

Eclipsing binary systems have in addition revealed that G and K supergiants possess extended chromospheres which could be detected outwards to $\sim$ 1 R_* (stellar radius) above the photospheres. Electron temperatures T_e and hydrogen ionization n_e/n_H seem to increase with height up to at least o.5 R_* ($n_e/n_H = 1o^{-2}$, $T_e = 1o^4$ K at o.5 R_*), and the winds start to be accelerated at heights above $\sim$ o.5 R_*.

Mass-loss rates appear to increase steeper than linearly with $L/g \cdot R$. It is shown that the observed mass-loss rates are consistent with stellar evolution constraints for both Pop. II and Pop I stars.

1. INTRODUCTION

The study of mass-loss from stars began in 1956 - before the detection of the solar wind - with Deutsch's spectroscopic observations of the α Her visual binary system.

Deutsch (1956) noticed that α Her (M5II), like other M (super) giants, has blue-shifted cores of strong resonance lines and that the same blue-shifted lines are seen in the spectrum of its G giant companion 5" apart. Since single G giants do not show sharp, blue-shifted resonance lines, Deutsch concluded that the M giant has a vast expanding envelope that encloses the companion, and that the line shifts in the line of sight of the companion are above the local escape velocity, i.e. circumstellar matter escapes the system.

As will be shown below, the binary technique of studying mass-loss of G to M giants and supergiants is a powerful tool to obtain accurate mass-loss rates and wind velocities as well as estimates of the wind temperature and information about the wind acceleration region. In particular, Zeta Aurigae binary systems are the only stars - besides the Sun - where the structure of the extended chromosphere and wind can be observed with high spatial resolution. For single stars, on the other

I. Appenzeller and C. Jordan (eds.), Circumstellar Matter, 307–318.

hand, it has turned out to be very difficult to determine mass-loss rates quantitatively from CS lines. The reason is that while it is possible to measure ion column densities N_{ion} and wind velocities v_w from a theoretical analysis of P Cyg type profiles superimposed upon the cores of strong resonance lines in stars like α Ori (c.f. Bernat and Lambert, 1976), it is not possible to infer from spectroscopic observations where in the line of sight the CS lines are formed, and since $\dot{M} = \text{const} \cdot N_{ion} \cdot v_w \cdot R_i$, where R_i is the inner shell radius, accurate mass-loss rates cannot be determined from optical observations of M giants and supergiants. The same difficulty - in addition to others - arises if one tries to determine mass-loss rates from circumstellar dust emission.

The only technique for measuring $\dot{M}$ at optical wavelengths appears to be spatially resolved imaging of CS shells in scattered resonance line photons like KI 7699 Å or NaD (Mauron et al. 1984, 1986). However, since the lines observed up to now are from minor ionization species, good knowledge of the ionization of metals and of the formation of CO is required. In particular, nonequilibrium effects (flow time ∿ recombination time scale) have to be taken into account. Reliable mass-loss rates are available now for α Ori and μ Cep (cf. Table 1).

2. VISUAL BINARIES

Deutsch (1956) invented the technique to determine the rate of mass-loss of a cool giant from CS absorption lines of a predominant ionization stage seen in the spectrum of a visual companion. By this technique one avoids the difficulty one has in single stars of locating the shell.

The visual binary technique has been applied to α Her (Reimers, 1977), α Sco (Kudritzki and Reimers, 1978) and - with less accuracy - to o Cet (Reimers and Cassatella, 1985).

Besides mass-loss rates and wind velocities (see Table 1) as inferred from the strengths of absorption lines seen in the spectrum of the companions, some additional information can be obtained from a study of excitation. In case of α Her, the observed absence of lines from excited fine structure levels of TiII ($N(a^4F_{5/2})/N(a^4F_{3/2}) < 0.15$) implies that the hydrogen particle density $n_H < 7.5 \cdot 10^4 cm^{-3}$ for T = 50 K and $n_H < 1.5 \cdot 10^4$ cm^{-3} for T >> 100 K. With a typical density of $n_H \approx 2 \cdot 10^4$ cm^{-3} as found from column densities, one can exclude T >> 100 K at a typical distance of 300 M giant radii. This is roughly in accordance with adiabatic cooling of the wind at large distances ($T \sim r^{-4/3}$).

In case of α Sco, the observed population of fine structure levels within the ground state of TiII which is due to electron collisions permits an independent estimate of the electron density in the wind (Kudritzki and Reimers, 1978).

https://doi.org/10.1017/S0074180900156608 Published online by Cambridge University Press

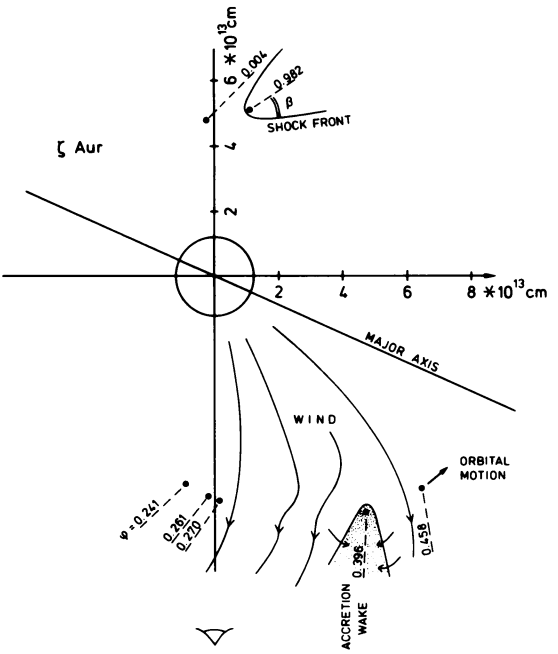

Figure 1. A roughly to-scale presentation of the accretion shock front and wake as observed for ζ Aur (from Che and Reimers, 1986).

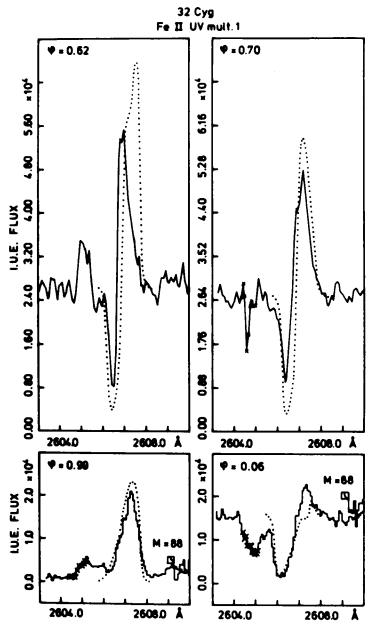

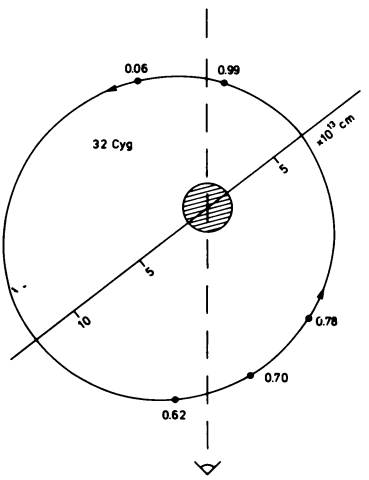

Figure 2. Location of B star relative to K supergiant at observed phases

Figure 3. Dependency of a wind line (Fe II UV Mult.1 resonance line) on phase (see Fig.2) in comparison with theory (....).

https://doi.org/10.1017/S0074180900156608 Published online by Cambridge University Press

3. ζ AUR/VV CEP TYPE BINARIES

With IUE, the optical separation of red giants with hot companions can be replaced by a separation through complementary energy distributions of the components. At IUE wavelengths, in particular in the short-wavelength range, one observes a pure B star spectrum upon which numerous CS P Cygni type lines formed in the extended wind and chromospheric absorption lines (near eclipse) of the red giant are superimposed.

The B star serves as an astrophysical light source (a "natural satellite") which moves around in the wind of the red giant. However, compared to widely separated visual binaries, a number of additional difficulties arise

- a non-spherical, 3-dimensional line transfer problem has to be solved since the light source (B star) is excentric from the wind symmetry center. Computer codes that solve this problem have been developed in the 2-level approximation by Hempe (1982, 1984) and for the multilevel case by Baade (1986)
- the wind is disturbed in the immediate surrounding of the B star as it moves supersonically through the wind and formes an accretion shock front (Chapman, 1981). However, a detailed study of the accretion shocks has shown that their geometrical size is very small compared to the CS shell (Fig.1) and can be neglected in line transfer calculations (Che-Bohnenstengel and Reimers, 1986)
- the hot B star ionizes the wind, i.e. an HII region is formed within the red giant wind. In 31 Cyg and α Sco, in particular, the size of the HII region is larger and it has to be taken into account quantitatively since ions like SiII and FeII which are used for the mass-loss rate determination may be doubly ionized within the HII regions.

On the other hand, ζ Aur binaries are the only stars besides the Sun where the winds and extended chromosphere can be studied with spatial (height) resolution.

3.1 Wind lines

The wind is visible at all phases in P Cyg type profiles (during total eclipse of B star pure emission lines) of ions like FeII, SiII, SII, MgII, CII, AlII, and oI. These lines are formed by scattering of B star photons in the wind of the red giant. A few wind lines like FeII Mult.9 (∿1275 Å) are seen in pure absorption due to the branching ratios of the upper levels which favour reemission as FeII UV Mult. 191 photons (Hempe and Reimers, 1982; Baade, 1986).

Theoretical modelling of wind line profiles and of their phase dependency has yielded accurate mass-loss rates and wind velocities for a number of systems (Table 1). It has turned out that a good mass-loss determination requires both phases with the B star in front of the red supergiant (which yields wind turbulence v_t) and phases with the B star behind the red supergiant(which yield the wind velocity v_w). Typically, $v_w \approx 2\ v_t$. Further details can be found in Che et al. (1983). It turned out that it was possible to match the circumstellar line profiles at all phases with <u>one</u> set of parameters v_w , v_t and - within a factor of 2 - one mass-loss rate $\dot{M}$ (Figs.2-5). This means that at least in the orbital

https://doi.org/10.1017/S0074180900156608 Published online by Cambridge University Press

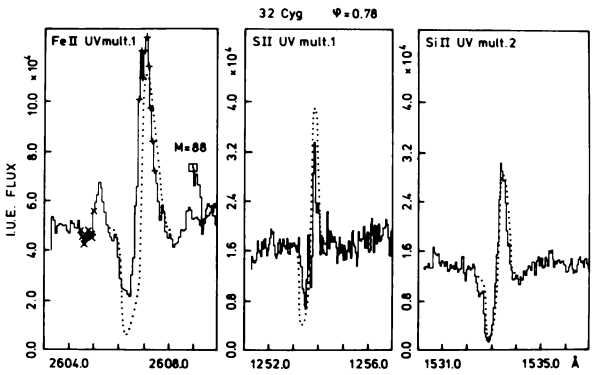

Figure 4. Comparison of theoretical (....) and observed wind line profiles for three ions (as for Fig. 2 and 3 from Che et al. 1983).

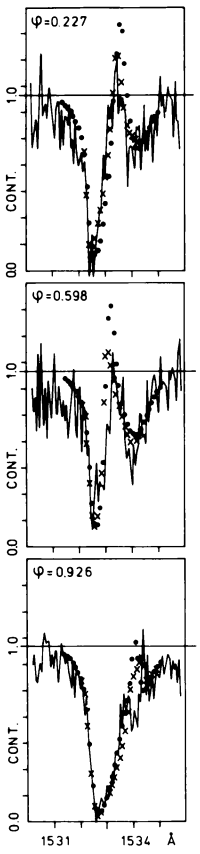

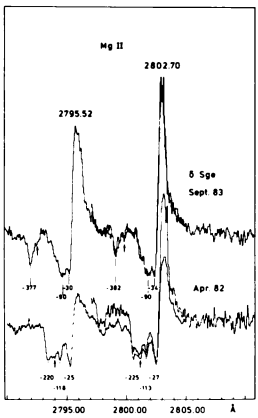

Figure 9. High velocity clouds in δ Sge (M2II, mean wind velocity ∿3o km/s) seen in the spectrum of its B star companion.

Figure 5. Observed and theoretical SiII UV Mult. 1 line at different phases for 22 Vul (G3Ib-II), from Reimers and Che-Bohnenstengel (1986).

https://doi.org/10.1017/S0074180900156608 Published online by Cambridge University Press

plane the envelope asymmetries (in density) are within a factor of 2 on a length-scale of several K giant radii. The example of α Sco shows that the influence of interstellar (IS) lines has to be considered carefully. As demonstrated in Fig.6 with SiII 1526 Å, all circumstellar o.oo eV lines in the spectrum of α Sco B suffer from IS absorption on the longward side of the profile (IS velocity is +5 km/s, Kudritzki and Reimers, 1978), i.e. the reemission part of the CS P Cyg profile appears absorbed at the resolution of IUE, while all other lines (like SiII 1533 Å) have the expected P Cyg profiles. Both v.d. Hucht et al. (198o) and Bernat (1981) used only the pure absorption lines to determine mass-loss rates which consequently came out too high by one order of magnitude with a scatter of a factor of ∿ 3o among rates from different ions. The correct treatment of the P Cyg profiles with Hempe's (1982) non-spherical line transfer code yields a mass-loss rate of ∿ $1o^{-6}$ $M_\odot$/yr (Hagen, 1984, Hagen et al. 1986), consistent with Hjellming and Newell's (1983) rate from radio emission from the HII region within the wind and with the rate from optical observations of TiII lines in α Sco B (Kudritzki and Reimers, 1978).

In case of 32 Cyg and 22 Vul, the wind electron temperature T_e could be estimated from the observed population of excited FeII levels. For 32 Cyg, at distances of more than 5 K giant radii, Che-Bohnenstengel (1984) found T_e = 48oo K for n_e/n_H = o.o1 and $T_e \gtrsim 1o^4$ K for smaller electron densities. The LTE value would be 42oo K. In 22 Vul, population of excited FeII levels is much higher, and a wind electron temperature of $3o \pm 1o \cdot 1o^4$ K was estimated with the assumption of pure electron collision excitation (Reimers and Che-Bohnenstengel, 1986). Such a high wind excitation is particularly remarkable in a star like 22 Vul which has common characteristics with 'hybrid atmosphere' stars like α Aqr : a high wind velocity, location in the HR diagram, it is a young intermediate mass star, and it has an extended chromosphere observed to 1 R_* above the photosphere during its 1985 eclipse (Schröder and Che-Bohnenstengel, 1985). However, since radiative excitation via high levels cannot be excluded at present, the high wind temperature of 22 Vul needs to be confirmed by improved theoretical techniques.

3.2 Chromospheric lines

The extended chromosphere - where the wind starts to expand - could be studied by means of the technique applied by O.C. Wilson, H.G. Groth, K.O. Wright and others in the 195os; and IUE data are a major advance in several respects: The B star provides a smooth continuum on which one observes numerous absorption lines up to heights (projected binary separations) of more than one supergiant radius above the photosphere. In addition to absorption lines, the wavelength and time dependence of totality in the UV (Fig.7) can be used for a density model of the inner chromosphere (Schröder 1985a, 1985b, 1986). Chromospheric densities could be represented by power laws of the form $\rho \sim r^{-2} \cdot h^{-a}$ with $a \gtrsim 2.5$ where r is the distance from the center of the star and h is the height above the photosphere. The empirical density distribution shows that after a steep decrease in the inner chromosphere already in the upper chromosphere (height > 1/2 to 1 giant star radii R_*) expansion

https://doi.org/10.1017/S0074180900156608 Published online by Cambridge University Press

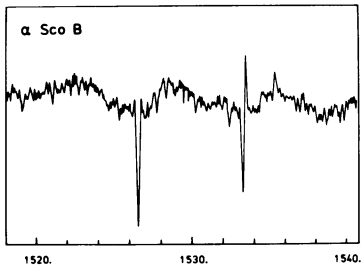

Figure 6. Interstellar absorption at SiII 1526 Å (o.oo eV) in comparison with the undisturbed wind line SiII 1533 Å (o.o1 eV).

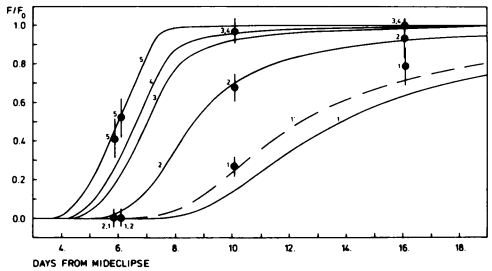

Figure 7. Light curves at 135o Å (1), 1513 (2), 1783 Å (3), 196o Å (4) and 2992 Å (5) during eclipse of 32 Cyg. Solid line represents best fit with model chromosphere (from Schröder, 1986).

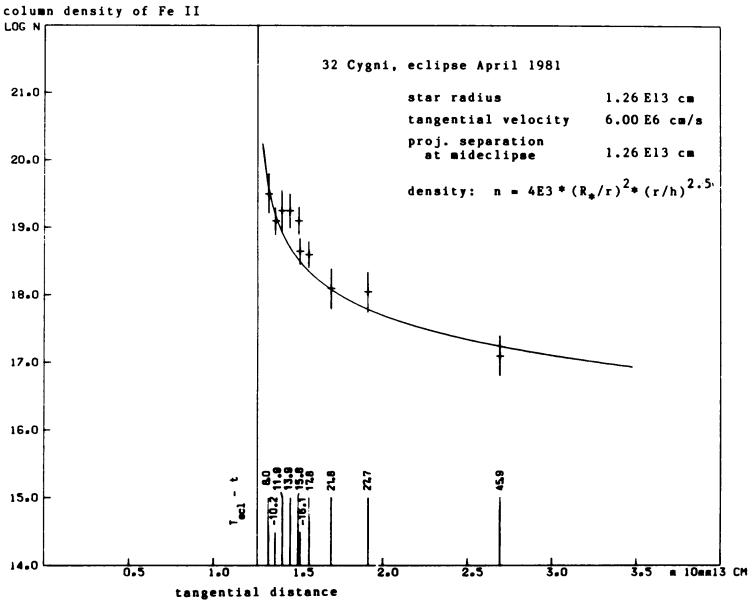

Figure 8. Chromospheric density distribution obtained from curve of growth analysis of ultraviolet FeII lines (Schröder, 1985a,b).

https://doi.org/10.1017/S0074180900156608 Published online by Cambridge University Press

starts ($\rho \sim r^{-2}$). A typical density at a height of 2 R_* is $1o^7$ cm^{-3} (Fig.8).

Since one observes total particle densities in the expanding chromosphere up to $h \lesssim 1.5\ R_K$, and in addition the wind density and velocity outside of $\sim 5\ R_K$, one can try to look for consistency by assuming a steady wind, i.e. to apply the equation of continuity. Using $\dot{M} = 4\ \pi\ r^2 \cdot \rho(r) \cdot v(r)$ and $\rho(r) = \rho_o \cdot (R_*/r)^2 \cdot (v/(r-R_*))^a$ for the chromosphere, we find $v(r) = \dot{M}\ (4\ \pi\ \rho_o R^2)^{-1} \cdot (1 - R_*/r)^a$ and a wind terminal velocity $v_\infty = \dot{M}\ (4\ \pi\ \rho_o \cdot R^2)^{-1}$ which can be checked with observed values for ρ_o, $\dot{M}$ and v_∞ for consistency. For 32 Cyg and 31 Cyg Schröder (1985) found consistency, which means that the empirical density distribution (when extrapolated by the equation of continuity to the outer wind) yields the correct mass-loss rate. In case of ζ Aur, the chromospheric density distribution was far too steep - at least at that particular limb position during eclipse - to give the mean mass-loss rate, which might be stellar analogue to a solar coronal hole.

Another stellar-solar analogue is the prominence detected during egress of the 1981 eclipse of 32 Cyg (Schröder, 1983). After egress from eclipse, an additional 'dip' in the light curve was seen at wavelengths $\lambda < 2ooo$ Å for at least 6 days. Since the observed "prominence" was optically thin, the observed frequency dependence of optical depths $\tau_\nu \sim \nu^{5.5}$ could be used to identify the opacity as Rayleigh scattering at HI ground state. A linear extension - perpendicular to the line of sight - of about 1/6 K giant radii ($\gtrsim 3o\ R_\odot$) and an apparent height of $\sim 15\ R_\odot$ above the limb (at 135o Å) was estimated from the light curves. The small observed velocity of +2o km/s as measured from a few absorption lines like VII 311o.7 or TiII 3o72 A seen in addition to the normal chromospheric lines indicates a slowly moving cloud. Also, even a moderate velocity perpendicular to the line of sight, e.g. a slow prominence moving upwards with the wind velocity of ∿ 6o km/s can be excluded, since within the 6 days the cloud was seen it would have moved by 45 $R_\odot$ (3 times the observed height above the limb). The density in the observed prominence was of the order of $1o^{12}$ cm^{-3}, about a factor of 1o higher than in the surrounding chromosphere. If the excess pressure was balanced by magnetic fields, a field strength of ∿ 4 Gauss would have been necessary.

Another finding important for our understanding of chromospheres and for the mass-loss mechanism operating in K supergiants is that the chromospheric electron temperature is $\sim 1o^4$ K with a tendency to increase with height, e.g. from $T_e \lesssim 85oo$ K at o.2 R_K above the photosphere to about 11 ooo K at o.5 R_K height in 32 Cyg. Hydrogen ionization appears to increase over the same range from about $n_e/n_H = 1o^{-3}$ to $1o^{-2}$ (Schröder, 1986). Both findings mean that extensive nonradiative heating occurs in heights above the photosphere where wind acceleration has started. At least in these stars, wind acceleration through radiation pressure on dust grains can be excluded as a possible mass-loss mechanism.

Although the extensive study of ζ Aur/VV Cep type stars with the IUE has brought a major advance in determining mass-loss rates of G to M supergiants and in understanding the structure of chromospheres, wind acceleration regions and winds of these stars, a number of difficulties

and problems must be overcome before wind acceleration can be understood in detail: (i) The S/N of single IUE spectra and the spectral resolution are not good enough for studying the wind acceleration region ($h \approx 1$ to 3 R_*). This difficulty can be overcome with the Hubble Space Telescope. (ii) The 3-dimensional line transfer code uses the Sobolev approximation for the source function which is not appropriate since v_w/v_t is not >> 1. (iii) Our wind temperature estimates neglected radiative transitions which may be important for FeII. Although a multilevel NLTE code has been developed (Baade, 1986), calculations involving 3-dimensional radiative transfer are not yet possible with so many levels as for FeII. (iv) Simple geometries have been used while inhomogeneities and departures from spherical outflow due to interactions with the companion have been neglected. In at least two stars (δ Sge, 32 Cyg) time variable high velocity components can be seen in the strongest wind lines. So, e.g. the M2II giant δ Sge with a mean wind velocity of $\approx$ 3o km/s, shows MgII 28oo components with velocities up to nearly 4oo km/s (Fig.9). While the high velocity clouds seem to contribute little to the total envelope mass, they may contribute to the energy budget of the wind. (v) A further difficulty arises through the presence of an early B star in the wind of the red giant. Within the HII region around the B star, Fe, e.g., is ionized a second time. Since in a system like 31 Cyg with a period of $\sim$1o yrs, where these effects are observed (Che et al. 1983), the HII region moves with the B star, and since the recombination time scale in the HI region is large compared to the orbital period, the FeII/FeIII ionization balance is probably not in detailed equilibrium.

4. MASS-LOSS RATES

Table 1 summarizes the results for 8 binary systems studied so far. In addition, mass-loss rates obtained for α Ori and μ Cep by means of the resonance line imaging technique by Mauron et al. (1984, 1985, 1986) are included since about the same accuracy as with the binary technique is achieved. Mass-loss rates for more stars and in particular more accurate values cannot be expected in the near future for normal giants. I shall therefore briefly discuss the implications for stellar evolution. Nearly all stellar evolution calculations which included mass-loss in the red giant stage have applied the semiempirical scaling law $\dot{M}\ (M_\odot/yr) = \eta \cdot 4.1o^{-13}\ L/g \cdot R$ (1) proposed on dimensional arguments and calibrated with empirical mass-loss rates for a number of Pop I giants and supergiants (Reimers, 1975). The dimensionless factor η $(1/3 \leq \eta \leq 3)$ has been introduced in order to take into account the then considerable uncertainty of mass-loss rates.

For this reason we test the simple scaling law with the improved empirical mass-loss rates.

In Fig.1o, the mass-loss rates from Table 1 are plotted versus $L/g \cdot R$. Two conclusions are evident

1) All observed mass-loss rates can be represented within realistic error bars (factors of 2 in both $\dot{M}$ and $L/g \cdot R$ to either side) by a relation $\dot{M} = 5 \cdot 1o^{-13}\ L/g \cdot R$. $(\eta = 1.25)$

2) The new empirical rates seem to indicate, however, a tendency for

https://doi.org/10.1017/S0074180900156608 Published online by Cambridge University Press

Table 1: Compilation of accurate mass-loss determinations

Star	Spectral Type	Technique	$\dot{M}$ (10^{-8} $M_\odot$/yr)	v_w (km/s)	v_t (km/s)	References
α^1Her	M5II	Vis.bin.	11	8	4	Reimers (1977)
α Sco A	M1Iab	Vis.bin.	7o	17		Kudritzki & R. (1978)
		Radio	2oo+)			Hjellming & Newell (1983)
		IUE	1oo	17	8	Hagen et al. (1986)
HR8752	GoIa	Radio	1ooo	3o		Lambert & Luck (1978)
ζ Aur	K4Ib	IUE	o.6	4o	3o	Che et al. (1983)
32 Cyg	K5Iab	IUE	2.8	6o	25	"
31 Cyg	K4Ib	IUE	$\sim$ 4	8o	2o	"
δ Sge	M2II	IUE	2	28	2o	Reimers & Schröder (1983)
22 Vul	G3II-Ib	IUE	o.6	16o	5o	Reimers & Che-B. (1986)
α Ori	M1.5Iab	KI				
		Image	2oo	1o		Mauron (1985)
μ Cep	M2Ia	NaD				
		Image	3ooo	47		Mauron et al. (1986)

+) With a mean molecular weight $\mu = 1.4$

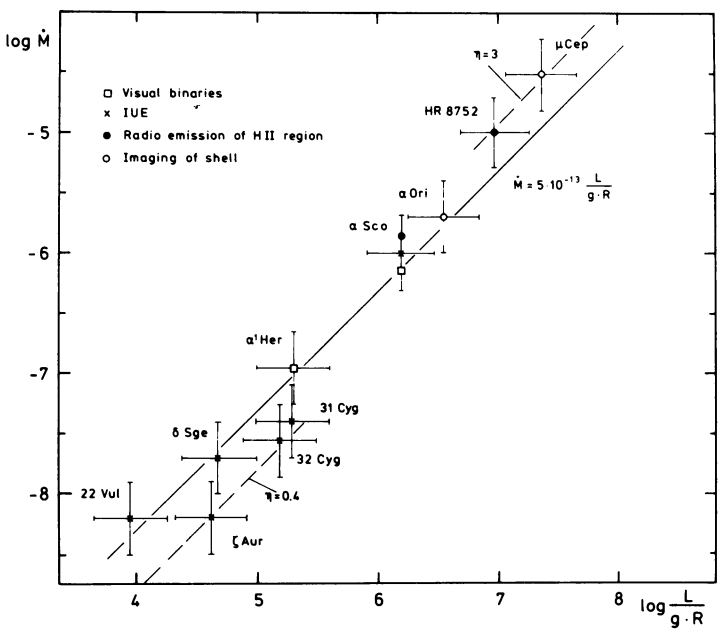

Figure 1o. Mass-loss rates $\dot{M}$ $(M_\odot/yr)$ for stars from Table 1 versus $L/g \cdot R$ (in solar units).

https://doi.org/10.1017/S0074180900156608 Published online by Cambridge University Press

a steeper dependence of mass-loss on luminosity, resp. $L/g \cdot R$.

A comparison of observed late stages of stellar evolution with evolutionary calculations applying red giant mass-loss in the simple parametrized form imposes constraints on η

i) Horizontal branch star masses and the observed upper luminosity limit of globular cluster AGB stars require $\eta \gtrsim 0.4$ (Renzini, 1977) for Pop.II stars

ii) The observed maximum initial mass for white dwarf progenitors M_{WD} as determined from white dwarf members of the intermediate age cluster NGC 2516 is $M_{WD} \gtrsim 8\ M_{\odot}$ or even higher (Reimers and Koester, 1982; Weidemann and Koester, 1983)

iii) Mass-loss rates of advanced AGB stars (OH-IR stars) seem to be higher by about an order of magnitude than predicted by the scaling law with $\eta = 1$ (Baud and Habing, 1983). Similarly, PN demand higher mass-loss rates if interpreted as excited winds of red giant progenitors.

Inspection of Fig.1o shows that for luminosities typical at the tip of the Pop.II AGB ($\log L \gtrsim 3.2$, $\log L/g \cdot R \gtrsim 5.3$), $\eta = 0.4$ does not contradict observations within realistic errors.

Similarly, for high luminosity $\eta = 3$ gives a good fit to observations. According to Iben and Renzini (1983), $\eta = 3$ would yield $M_{WD} \gtrsim 1o$. However, observations at high luminosities in Fig.1o are from massive stars and should not be extrapolated deliberately to advanced evolutionary stages of intermediate mass stars. For such stars, Baud and Habing have proposed a parametrization of observations of mass-loss from OH-IR stars in the form

$$\dot{M}(t) = \mu \cdot \frac{L \cdot R}{M_e(t)} \quad \text{where } \mu = \frac{M_e}{M}\, 4 \cdot 1o^{-13} \quad \text{and } M_e(t) \text{ is the envelope mass}$$

instead of the total mass. This modified relation gives about the same rates for most of the AGB lifetime as relation (1), while at the end of the AGB phase the reduced envelope mass leads to a steep increase of mass-loss rates, in accordance with observational requirements.

In conclusion, mass-loss rates accurately determined with the binary technique are in full agreement with stellar evolution constraints. However, a semiempirical fit of mass-loss rates with $\dot{M} \sim L/g \cdot R$ (or $\dot{M} \sim (L/g \cdot R)^{1.3}$ as might be derived from Fig.1o) should not be extrapolated to stars of distinctly different properties like OH-IR stars with thick dust shells, F stars, carbon stars etc.

ACKNOWLEDGEMENT: This paper is based on the work of the 'binary wind team' at Hamburg Observatory, R. Raade, A. Che-Bohnenstengel, K. Hempe, K.-P. Schröder and K. Schönberg. The Deutsche Forschungsgemeinschaft supported the binary project with several grants to the author.

REFERENCES

Baade,R. 1986, Astron.Astrophys. 154, 145
Baud,B., Habing,H.J. 1983, Astron.Astrophys. 127, 73
Bernat,A.P. 1981, Ap.J. 252, 644
Chapman,R.D. 1981, Ap.J. 248, 1o43
Che-Bohnenstengel,A. 1984, Astron.Astrophys. 138, 333
Che,A., Hempe,K., Reimers,D. 1983, Astron.Astrophys. 126, 225
Che,A., Reimers,D. 1983, Astron.Astrophys. 127, 227
Che-Bohnenstengel,A., Reimers,D. 1986, Astron.Astrophys. 156, 172
Deutsch,A.J. 1956, Ap.J. 123, 21o
Hagen,H.J. 1984, Diplomarbeit Universität Hamburg
Hagen,H.J., Hempe,K., Reimers,D. 1986, Astron.Astrophys. in preparation
Hempe,K., 1982, Astron.Astrophys. 115, 133
1984, Astron.Astrophys.Suppl. 56, 115
Hempe,K., Reimers,D. 1982, Astron.Astrophys. 1o7, 36
Hjellming,R.M., Newell,R.T. 1983, Ap.J. 275, 7o4
Iben,I., Renzini,A. 1983, Ann.Rev.Astr.Ap. 21, 271
Kudritzki,R.-P., Reimers,D. 1978, Astron.Astrophys. 7o, 227
Lambert,D.L., Luck,R.E. 1978, M.N.R.A.S. 184, 55
Mauron,N. 1985, Doct.Thesis, Univ. Toulouse
Mauron,N., Fort,B., Querci,F., Dreux,M., Fauconnier,T., Lamy,P. 1984
Astron.Astrophys. 13o, 341
Mauron,N., Cailloux,M., Prieur,J.L., Pilloles,P., Lefèvre,O. 1986,
Astron.Astrophys. in press
Reimers,D. 1975, Mem.Soc.Roy.Sci. Liège 6e Ser. 8, 369
Reimers,D. 1977, Astron.Astrophys. 61, 217 (Erratum 67, 161)
Reimers,D., Koester,D. 1982, Astron.Astrophys. 116, 341
Reimers,D., Schröder,K.-P. 1983, Astron.Astrophys. 124, 241
Reimers,D., Cassatella,A. 1985, Ap.J. 297, 275
Reimers,D., Che-Bohnenstengel,A. 1986, Astron.Astrophys. in press
Renzini,A. 1977, In "Advanced Stages of Stellar Evolution" (eds.
P. Bouvier, A. Maeder), Geneva p. 151
Schröder,K.-P. 1983, Astron.Astrophys. 124, L16
Schröder,K.-P. 1985a, Astron.Astrophys. 147, 1o3
1985b, Ph.D.Thesis University of Hamburg
1986, Astron.Astrophys. in press
Schröder,K.P., Che-Bohnenstengel,A. 1985, Astron.Astrophys. (Letters)
151, L5
v.d.Hucht,K., Bernat,A.P., Kondo,Y. 198o, Astron.Astrophys. 82, 14
Weidemann,V., Koester,D. 1983, Astron.Astrophys. 121, 77